Spectroscopic and Enzymatic Characterization of the Active Site Dinuclear Metal Center of Calcineurin: Implications for a Mechanistic Role†

Lian Yu,‡ John Golbeck,§ Janet Yao,‡ and Frank Rusnak*,‡

Section of Hematology Research and Department of Biochemistry and Molecular Biology, Mayo Clinic and Foundation, Rochester, Minnesota 55905, and Department of Biochemistry and Molecular Biology, Pennsylvania State University, University Park, Pennsylvania 16802

Received March 6, 1997; Revised Manuscript Received June 12, 1997⊗

ABSTRACT: The active site of bovine brain calcineurin contains an $Fe^{3+}-Zn^{2+}$ dinuclear metal center. Replacement of Zn^{2+} with Fe^{2+} yields a mixed valence $Fe^{3+}-Fe^{2+}$ center that exhibits a characteristic EPR signal that can be used as a convenient spectroscopic probe of the active site. Addition of product phosphate to both the $Fe^{3+}-Fe^{2+}$ and $Fe^{3+}-Zn^{2+}$ forms of calcineurin led to perturbations of the respective EPR signals, indicating that phosphate affects the environment of the paramagnetic centers. Anaerobic titrations of the iron-substituted $Fe^{3+}-Fe^{2+}$ enzyme with dithionite resulted in a gradual loss of activity toward *p*NPP that paralleled the loss of intensity of the EPR signal of the mixed valence diiron center. During dithionite reduction, an EPR resonance with $g \approx 12$ appeared. The intensity of this resonance increased when the spectrum was recorded in a parallel mode cavity and was therefore attributed to a paramagnetic center with integer spin. Oxidation of the $Fe^{3+}-Fe^{2+}$ cluster to the diferric state by hydrogen peroxide also led to a loss of activity. These results indicate that the mixed valence oxidation state represents the catalytically competent form of the cluster. The dependence of the enzyme activity on the redox state of the cluster has implications for a mechanistic role.

The metalloprotein phosphatases are a family of metalloenzymes capable of hydrolyzing a variety of phosphate esters (Lohse et al., 1996; Rusnak et al., 1996). The best characterized members of this family are the plant and mammalian purple acid phosphatases, enzymes which utilize either $Fe^{3+}-Fe^{2+}$ or $Fe^{3+}-Zn^{2+}$ active site dinuclear metal cofactors (Kurtz, 1990; Vincent et al., 1990). Recently this family has been expanded to include the eukaryotic serine/threonine protein phosphatases 1 (PP1),[1] 2A (PP2A), and 2B (PP2B, calcineurin). These protein phosphatases are involved in eukaryotic signal transduction pathways that hydrolyze phosphoserine and phosphothreonine groups that are part of polypeptide chains (Shenolikar & Nairn, 1991). Other members include various bacterial proteins (Lohse et al., 1996), and the bacteriophage lambda protein phosphatase (Zhuo et al., 1993; Zhuo et al., 1994).

The hallmark of enzymes in this family is the phosphoesterase motif, **D**X**H**$(X)_n$G**D**XXD$(X)_m$G**N**HD/E (Koonin, 1994; Lohse et al., 1996). Recent crystallographic studies of purple acid phosphatase (Sträter et al., 1995; Klabunde et al., 1996), PP1 (Goldberg et al., 1995; Egloff et al., 1995), and calcineurin (Griffith et al., 1995; Kissinger et al., 1995) have determined that the phosphoesterase motif is represented at the secondary level as a $\beta-\alpha-\beta-\alpha-\beta$ fold that serves to position two metal ions at the active site with four of the metal ligands provided by loop residues between each β-sheet and α-helix (boldface residues noted in the phosphoesterase motif above).[2] The importance of this motif in structure/function has been confirmed by mutagenesis studies of PP1 and lambda protein phosphatase which have altered the various metal ligands and found substantial decreases in k_{cat} yet little change in substrate K_m (Zhuo et al., 1994; Zhang et al., 1996).

The two metal ions of the active site, designated as M1 and M2 in the three-dimensional structure of PP1 (Goldberg et al., 1995), form a carboxylate- and solvent-bridged dinuclear metal center with spacing between metal ions of approximately 3−4 Å (Rusnak et al., 1996). Various metal ions can apparently be accommodated by the $\beta-\alpha-\beta-\alpha-\beta$ fold although there are a few systematic studies which have identified either the physiologic metal ions or the most catalytically efficient ones. In the purple acid phosphatases, the $Fe^{3+}-Fe^{2+}$ and $Fe^{3+}-Zn^{2+}$ forms have been characterized and appear to have nearly identical catalytic activities (Keough et al., 1980; Antanaitis et al., 1980). In these enzymes, the Fe^{3+} ion is situated in the M1 site as evidenced by the presence of a tyrosine-to-Fe^{3+} charge transfer band in the 500−550 nm region of the visible spectrum (Kurtz,

†This work was supported by a grant from the National Institutes of Health (GM46865 to F.R.).

* To whom correspondence should be addressed at Mayo Clinic and Foundation, 200 First St. S.W., Rochester, MN 55905. Telephone: (507) 284-4743. Fax: (507) 284-8286. Email: rusnak@mayo.edu.

‡ Mayo Clinic and Foundation.

§ Pennsylvania State University.

⊗ Abstract published in *Advance ACS Abstracts,* August 15, 1997.

[1] Abbreviations: BME, β-mercaptoethanol; DTT, dithiothreitol; EPR, electron paramagnetic resonance; MOPS, 3-(*N*-morpholino)propanesulfonic acid; *p*NPP, *p*-nitrophenyl phosphate; PP1, protein phosphatase 1; PP2A, protein phosphatase 2A; PP2B, protein phosphatase 2B (calcineurin).

[2] The motif in the plant and mammalian purple acid phosphatases, **D**$(X)_n$G**D**XX**Y**$(X)_m$G**N**HD/E, represents a variation of the phosphoesterase motif. Noteworthy differences include the absence of a histidine residue in the loop between the first β-sheet/α-helix and the presence of a tyrosine residue in the loop between the second β-sheet/α-helix. These substitutions as well as the presence of an additional histidine ligand outside the $\beta-\alpha-\beta-\alpha-\beta$ motif yield a net replacement of a water (hydroxide) ligand with a tyrosine residue in the coordination sphere of the dinuclear metal center of purple acid phosphatases (Rusnak et al., 1996).

S0006-2960(97)00519-9 CCC: $14.00

1990; Vincent et al., 1990). Besides Fe^{2+} and Zn^{2+}, the M2 site in purple acid phosphatase has been shown to bind a number of other divalent metals such as Cu^{2+}, Hg^{2+}, and Co^{2+} (Beck et al., 1984; Holz et al., 1992). Biochemical and spectroscopic studies of purified bovine calcineurin also indicate the presence of an active site dinuclear $Fe^{3+}-Zn^{2+}$ center which has been modeled into the corresponding M1 and M2 sites based on a comparison with purple acid phosphatase (King & Huang, 1984; Rusnak et al., 1996). As with purple acid phosphatases, the Zn^{2+} ion of calcineurin can be replaced with Fe^{2+} to yield a mixed valence $Fe^{3+}-Fe^{2+}$ diiron cluster that exhibits a characteristic EPR resonance with $g_{av} < 2.0$ and has a comparable phosphatase activity to the $Fe^{3+}-Zn^{2+}$ form (Yu et al., 1995). The dinuclear metal center of mammalian PP1 is less well characterized but was modeled to accommodate either two Mn^{2+} ions (Goldberg et al., 1995) or an $Fe^{2+}-Mn^{2+}$ cluster (Egloff et al., 1995). The presence of Mn^{2+} is likely since it was included in the purification and/or crystallization buffers, but whether it was bound in one or both sites was not firmly established, nor was the oxidation state of the bound iron atom determined.

In this study, we have used EPR spectroscopy to further define the role of the dinuclear metal center of calcineurin. Addition of product phosphate to both the $Fe^{3+}-Zn^{2+}$ and $Fe^{3+}-Fe^{2+}$ forms of calcineurin demonstrates that both metal clusters are perturbed by phosphate binding. Furthermore, incremental additions of dithionite to the $Fe^{3+}-Fe^{2+}$ form lead to a loss of the associated EPR signal, a parallel decrease in enzyme activity, and concomitant formation of a $g \approx 12$ signal due to an integer spin resonance. Oxidation of the $Fe^{3+}-Fe^{2+}$ cluster to the diferric state by hydrogen peroxide also resulted in a decrease in activity. These results indicate that the oxidation state required for activity in the iron-substituted enzymes is the $Fe^{3+}-Fe^{2+}$ state and establish a role for the cluster in the catalytic mechanism of phosphate ester hydrolysis.

EXPERIMENTAL PROCEDURES

Materials. Hydrogen peroxide, *p*-nitrophenyl phosphate, $Fe(NH_4)_2(SO_4)_2$, β-mercaptoethanol, DEAE-Sepharose CL-6B, and Sephacryl S-300 were purchased from Sigma (St. Louis, MO). Calmodulin was purified from bovine brain as described (Dedman & Kaetzel, 1983). PM30 and YM3 ultrafiltration membranes were purchased from Amicon (Beverly, MA). NAP 25 gel filtration columns were purchased from Pharmacia Biotech (Piscataway, NJ).

Methods. Protein concentrations were measured using the Pierce (Rockford, IL) protein assay reagent and bovine serum albumin as a standard (Bradford, 1976).

Purification of Bovine Brain and Recombinant Rat Calcineurin. Bovine brain calcineurin was isolated as described (Klee et al., 1983) and used as the source of $Fe^{3+}-Zn^{2+}$ (native) calcineurin. Recombinant rat calcineurin A was expressed in *E. coli*, reconstituted with myristoylated recombinant rat calcineurin B, and purified to homogeneity as described (Sikkink et al., 1995). Recombinant calcineurin was used for all iron reconstitution studies.

Anaerobic Assays of Calcineurin Phosphatase Activity. Calcineurin phosphatase activity was measured using *p*NPP as substrate by following the increase in absorbance at 410 nm as described (Sikkink et al., 1995). For anaerobic assays, a septum-sealed 500 μL quartz UV/visible cuvette containing 25 mM MOPS, 0.1 mM $CaCl_2$, pH 7.0, 1 μM calmodulin, and 10 mM *p*NPP was made anaerobic by repetitive backflushing with oxygen-free argon. After incubating for 2−5 min at 30 °C, the reaction was initiated by the addition of an anaerobic solution of calcineurin. Activity was measured by following the increase in absorbance at 410 nm using $\Delta\epsilon_{410} = 7180\ M^{-1}\ cm^{-1}$. Initial velocities were obtained from the slope of the progress curves during the first ≈20−25 s following addition of enzyme.

Preparation of Iron-Substituted Calcineurin. The mixed valence $Fe^{3+}-Fe^{2+}$ oxidation state of calcineurin was prepared according to a modification of the published procedure (Yu et al., 1995). Briefly, recombinant calcineurin was added to a final concentration of 6.4 μM to a solution of 100 mM Tris-HCl, 710 mM BME, pH 7.5. After 5 min, an anaerobic solution of 30 mM $Fe(NH_4)_2(SO_4)_2$ was added slowly to a final concentration of 0.375 mM, and the reaction mixture was incubated at 4 °C for 12 h. The protein was then concentrated using an Amicon PM30 centricon and buffer-exchanged by passage over a NAP25 column equilibrated with 100 mM Tris-HCl, 1 mM BME, pH 7.5. Following buffer exchange, the sample was concentrated, transferred to a quartz EPR cuvette, and frozen in liquid nitrogen.

The sample of calcineurin exhibiting the integer spin $g \approx 12$ EPR resonance used for parallel versus perpendicular mode EPR (Figure 6) was prepared in an identical fashion except that the reconstituted protein solution was buffer-exchanged into 100 mM Tris-HCl, 100 mM BME, pH 7.5.

Phosphate Complexes of Native and Iron-Substituted Calcineurin. A stock solution of 0.5 M potassium phosphate, pH 7.5, was added to a final concentration of 20 mM to EPR samples of both native ($Fe^{3+}-Zn^{2+}$) and iron-substituted mixed valence ($Fe^{3+}-Fe^{2+}$) calcineurin. Anaerobic conditions were maintained during addition using a cell similar to one described previously to prevent oxidation to the diferric oxidation state (Averill et al., 1978).

Dithionite Titrations of the Mixed Valence State of Calcineurin. At the beginning of the experiment, 250 μL of iron-substituted calcineurin (260 μM) in 100 mM Tris-HCl, 1 mM BME, pH 7.5, was placed in an EPR cuvette using the anaerobic cell described above. Following initial characterization by EPR, the sample was thawed under anaerobic conditions. Aliquots of a solution of 10 mM sodium dithionite ($Na_2S_2O_4$) were added directly to the sample using a Hamilton gas-tight syringe. After a 2 min incubation at room temperature, 2 μL of the sample was transferred anaerobically to a septum-sealed UV/vis cuvette for assay using *p*NPP while the remainder of the sample was frozen in liquid nitrogen for analysis by EPR spectroscopy. This process was repeated for each serial addition of dithionite.

Oxidation of the Mixed Valence State of Calcineurin by H_2O_2. Oxidation of calcineurin with hydrogen peroxide was carried out anaerobically by addition of a solution of 20 mM H_2O_2 directly to the EPR sample. At the beginning of the experiment, 250 μL of iron-substituted calcineurin (150 μM) in 100 mM Tris-HCl, 1 mM BME, pH 7.5, was added to an EPR cuvette using the anaerobic cell as described above. Following initial characterization by EPR, the sample was thawed under anaerobic conditions, and an aliquot of H_2O_2 was added using a Hamilton gas-tight syringe. After a 2

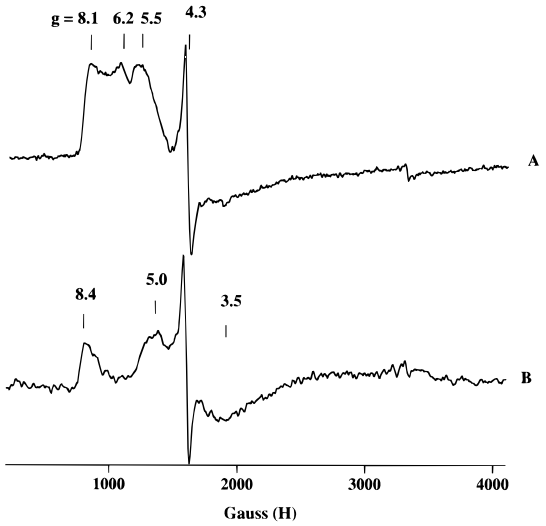

FIGURE 1: EPR spectra of the $Fe^{3+}-Zn^{2+}$ form of bovine brain calcineurin in the absence (A) and presence (B) of 20 mM NaH_2PO_4. The EPR samples contained 510 μM calcineurin in (A) and 260 μM in (B). The buffer for both samples was 20 mM Tris-HCl, 0.1 mM EDTA, 1.0 mM magnesium acetate, 1.0 mM DTT, 0.15 M KCl, pH 7.5. A base line EPR spectrum of buffer alone has been subtracted from each spectrum. Spectrometer conditions were the following: temperature, 5.0 K in (A) and 4.8 K in (B); microwave frequency, 9.2334 GHz in (A) and 9.2357 GHz in (B); modulation amplitude, 10 G at 100 kHz; microwave power, 0.16 mW.

min incubation at room temperature, 2 μL of sample was transferred anaerobically to a septum-sealed UV/vis cuvette for assay using *p*NPP while the remainder was frozen in liquid nitrogen for analysis by EPR spectroscopy. This process was repeated for each serial addition of hydrogen peroxide.

Electron Paramagnetic Resonance Spectroscopy. EPR studies were performed on a Bruker ESP300E spectrometer operating at 9 GHz (X-band) microwave frequency and equipped with an Oxford Instruments ESR 900 continuous flow cryostat for temperature regulation. EPR spectra of native ($Fe^{3+}-Zn^{2+}$) bovine calcineurin with and without phosphate were recorded on a Varian E109 spectrometer equipped with an Oxford Instruments ESR 910 cryostat in the lab of Dr. J. D. Lipscomb at the University of Minnesota. Parallel mode spectra were recorded using a Bruker ECS-106 spectrometer using a bimodal resonator operating at either 9.65 GHz (perpendicular mode) or 9.35 GHz (parallel mode).

Spin quantitations of the EPR resonances due to the mixed valence EPR resonance were performed using EDTA·Cu^{2+} as a standard as described (Yu et al., 1995). The concentration of the EDTA·Cu^{2+} was determined by Cu analysis using inductively coupled plasma emission spectrometry. Corrections for integrated intensities of sample versus standard were carried out according to Aasa and Vänngård (1975).

RESULTS

Effect of Phosphate on Native Calcineurin. Figure 1 shows the low-temperature EPR spectra of native bovine calcineurin in the presence and absence of 20 mM phosphate. In the absence of phosphate (Figure 1A), the spectrum is complex and not fully resolved. Most notable are features at $g = 8.1$, 6.2, 5.5, and 4.3 which result from high-spin ferric ions ($S = {}^5/_2$), possibly in three different ligand environments. The EPR spectra of high-spin ferric ions can be described by the spin Hamiltonian (H_e) (eq 1):

$$H_e = D[S_z^2 - {}^1/_3 S(S+1) + E/D(S_x^2 - S_y^2)] + g_o\beta\,\mathbf{S}\,\mathbf{H} \quad (1)$$

In eq 1, D and E are the zero-field splitting parameters, g_o is the intrinsic g-value, and H is the applied magnetic field. In the absence of an applied magnetic field, the ground state of the ferric ion is split into three Kramers doublets by the zero-field splitting term in eq 1. For applied magnetic fields such that $\beta H \ll |D|$, the observed g-values depend upon the value of the rhombicity parameter, E/D. Thus, the sharp derivative feature at $g = 4.3$ results from a species with $E/D = {}^1/_3$ and is due to a small amount of adventitious iron bound to the protein. For $D > 0$ and $E/D \approx 0.11$, the $\pm{}^1/_2$ Kramers ground doublet of an $S = {}^5/_2$ system would yield an EPR spectrum with g-values of 8.1, 3.5, and 1.7. The positive feature at $g = 8.1$ may represent one of these resonances while the resonances at 3.5 and 1.7 cannot be resolved in the spectrum of Figure 1A. The feature at $g = 8.1$ decreases in intensity with increasing temperature, consistent with a ground state assignment. The temperature and power saturation behavior of the features at $g = 6.2$ and 5.7 are roughly parallel yet vary slightly compared the behavior of the $g = 8.1$ feature (data not shown), suggesting that they may be due to a high-spin Fe^{3+} ion with near axial symmetry. The spectra remain broad and unresolved in the temperature range 2.5−30 K (data not shown). Therefore, a definite assignment of the electronic origin of these resonances is difficult, rendering spin quantitations of these species unfeasible.

Upon addition of phosphate, the EPR spectrum of the $g = 4.3$ component is unaffected, affirming its assignment as adventitious iron (Figure 1B). Phosphate affected the spectrum of the major high-spin Fe^{3+} specie(s) such that features with g-values of 8.4, 5.0, and 3.5 are now observed. The fact that product phosphate altered the EPR spectrum indicates that the environment of the ferric ion is perturbed.

Effect of Phosphate on Iron-Substituted Calcineurin. The EPR spectrum of recombinant rat calcineurin containing a mixed valence $Fe^{3+}-Fe^{2+}$ cluster is shown in Figure 2A. The EPR spectrum with g-values of 1.93, 1.77, and 1.64 is identical to the spectrum of iron-substituted bovine calcineurin prepared by replacing the Zn^{2+} ion with Fe^{2+} (Yu et al., 1995). The signal arises from transitions between a ground state doublet with $S = {}^1/_2$ due to antiferromagnetic coupling between the high-spin Fe^{3+} ($S_1 = {}^5/_2$) and high-spin Fe^{2+} ($S_2 = 2$) ions of the binuclear metal center. At 3.6 K, the signal becomes saturated above 25 mW and completely disappears for $T > 20$ K (Figure 2B,C).

Upon addition of 20 mM phosphate, the EPR spectrum shown in Figure 2A is replaced by a new signal with g-values of 1.98, 1.70, and 1.44 (Figure 3A). Besides the shifts in resonance positions, several other differences are observed between the signal in the presence versus absence of phosphate. Besides being weaker in intensity, the signal in the presence of phosphate is significantly broadened, difficult to saturate at 3.6 K (Figure 3B), and disappears for $T \geq 12$ K (Figure 3C). All of these features indicate a weaker exchange coupling between the Fe^{3+} and Fe^{2+} ions compared to the EPR signal in the absence of phosphate.

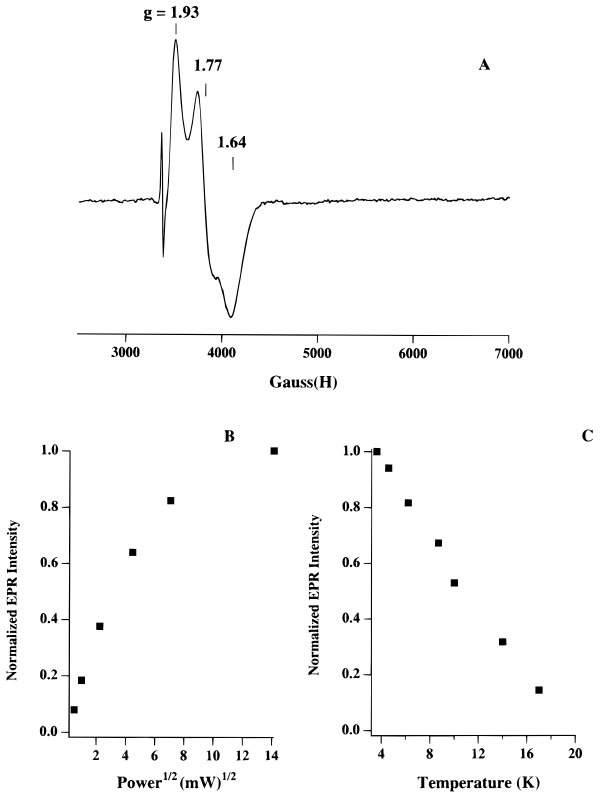

FIGURE 2: Temperature and microwave power dependence of the EPR spectrum of mixed valence ($Fe^{3+}-Fe^{2+}$) iron-substituted calcineurin. The 250 μL sample contained 180 μM calcineurin in 100 mM Tris-HCl, 1 mM BME, pH 7.5. A base line spectrum of buffer alone has been subtracted. Spectrometer conditions: temperature, 3.6 K; microwave frequency, 9.438 GHz; modulation amplitude, 10 G at 100 kHz. (A) 3.6 K EPR spectrum of iron-substituted calcineurin; microwave power, 20 mW. (B) Dependence of the EPR signal shown in (A) on microwave power; temperature = 3.6 K. (C) Plot of EPR signal intensity versus temperature from 3.6 to 17 K; microwave power = 20 mW.

Calcineurin Phosphatase Activity Using pNPP as Substrate. In the presence of Ca^{2+} and calmodulin but in the absence of $MnCl_2$, bovine brain calcineurin undergoes rapid inactivation using pNPP as substrate. In contrast, the time course of product formation in the presence of $MnCl_2$ remains linear over several minutes (Pallen & Wang, 1983). Similar kinetic behavior is observed using the $Fe^{3+}-Fe^{2+}$ form of calcineurin (Figure 4).[3] The presence of Mn^{2+} in assay buffers, however, complicates experiments investigating the effect of the bound Fe ions on enzyme activity since Mn^{2+} might exchange for one or both of these ions during the course of the assay. In order to assess calcineurin phosphatase activity, the rate of *p*NPP hydrolysis during the early stage of the reaction ($t \leq 25$ s) was measured. During this period, the velocity of the reaction in the absence of

[3] During the first 30 s of the assay, the amount of *p*-nitrophenol formed corresponds to 7.2 μM, or approximately 23 turnovers given the amount of calcineurin in the assay (0.32 μM). Therefore, the nonlinear velocity curves do not represent the breakdown of an intermediate (e.g., a phosphoenzyme intermediate) but are more characteristic of a time-dependent inactivation process with an estimated half-life of approximately 1−2 min. Slow binding product inhibition by either phosphate or *p*-nitrophenol can also be ruled out since preincubation of enzyme with either of these had no effect on progress curves. The rate of inactivation is dependent upon the substrate concentration indicating substrate inhibition (data not shown). The mechanism of this process is not yet understood but may involve metal ion displacement (Pallen & Wang, 1984, 1986; Rao & Wang, 1989).

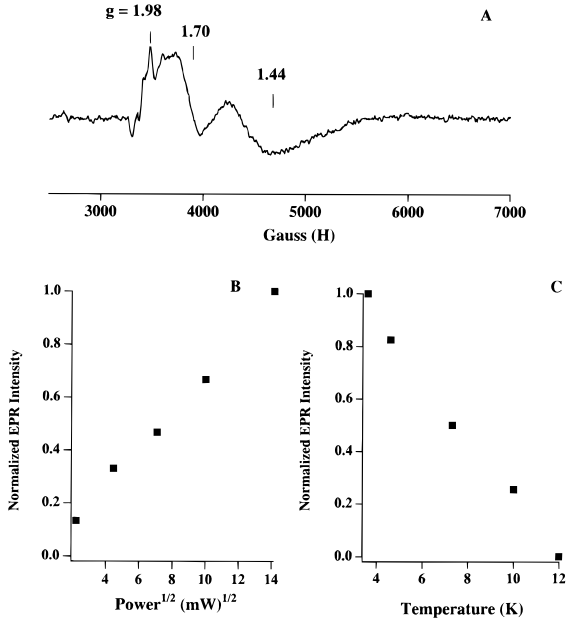

FIGURE 3: Temperature and microwave power dependence of the EPR spectrum of the phosphate complex of mixed valence ($Fe^{3+}-Fe^{2+}$) iron-substituted calcineurin. The 250 μL sample contained 180 μM calcineurin in 100 mM Tris-HCl, 1 mM BME, pH 7.5. A base line spectrum of buffer alone has been subtracted. The feature near $g = 1.98$ represents an artifact of base line subtraction. Spectrometer conditions: temperature, 3.6 K; microwave frequency, 9.438 GHz; modulation amplitude, 10 G at 100 kHz. (A) 3.6 K EPR spectrum of iron-substituted calcineurin following the addition of 20 mM potassium phosphate; microwave power, 20 mW. (B) Dependence of the EPR signal shown in (A) on microwave power; temperature = 3.6 K. (C) Plot of EPR signal intensity versus temperature from 3.6 to 17 K; microwave power = 20 mW.

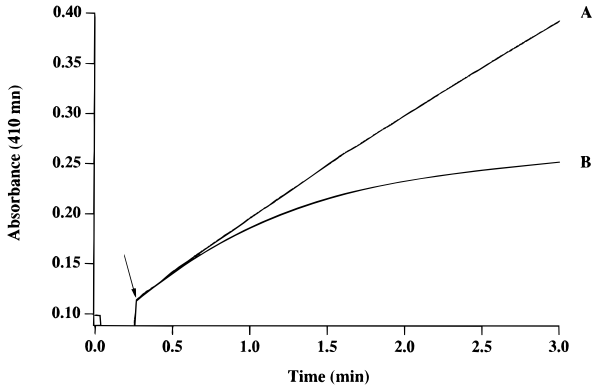

FIGURE 4: Mixed valence calcineurin *p*NPP activity in the presence and absence of $MnCl_2$. Iron-substituted $Fe^{3+}-Fe^{2+}$ calcineurin (0.32 μM) was added (at time indicated by arrow) to a solution of 20 mM MOPS, 0.1 mM $CaCl_2$, 1.0 μM calmodulin, 1.0 mM DTT, and 10 mM *p*NPP. The formation of product *p*-nitrophenol followed as a function of time at 410 nm (B). In (A), 1.0 mM $MnCl_2$ was included in assay buffers.

$MnCl_2$ is identical to the steady-state Mn^{2+}-dependent rate (Figure 4). Thus, the rate of *p*NPP hydrolysis in the presence of only Ca^{2+} and calmodulin corresponds to a specific activity of 0.58 ± 0.027 μmol min^{-1} mg^{-1} while in a parallel assay including 1.0 mM Mn^{2+} in the buffer, the rate was 0.57 ± 0.013 μmol min^{-1} mg^{-1}.

Dithionite Titrations of the Mixed Valence State of Calcineurin and Correlation with Phosphatase Activity. Sodium dithionite was anaerobically titrated into a sample of calcineurin prepared in the mixed valence ($Fe^{3+}-Fe^{2+}$) oxidation state to reduce the ferric ion and determine the

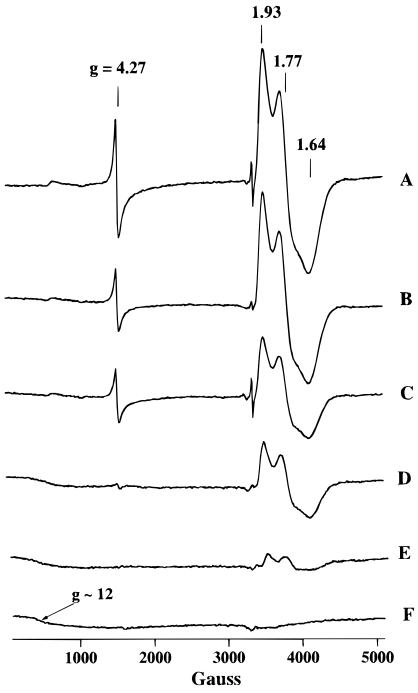

FIGURE 5: EPR spectra at 3.6 K of mixed valence iron-substituted calcineurin in the absence (A) and presence of various concentrations of dithionite (B−F). The concentrations of dithionite were 0.0 mM in (A), 0.24 mM in (B), 0.64 mM in (C), 1.1 mM in (D), 1.6 mM in (E), and 2.1 mM in (F). The samples contained 260 μM iron-substituted calcineurin and 50 mM Tris-HCl, 1 mM BME, pH 7.5. Spectrometer conditions: microwave frequency, 9.443 GHz; modulation amplitude, 10 G at 100 kHz; microwave power, 20 mW. The arrow indicates the position of the $g \approx 12$ resonance that appears upon dithionite reduction.

Table 1: Correlation between Calcineurin Activity and the Intensity of the Mixed Valence $Fe^{3+}-Fe^{2+}$ EPR Signal during Sodium Dithionite Reduction

$[Na_2S_2O_4]$, mM	signal intensity spins per protein (% of untreated)	calcineurin *p*NPP act., units[a] (% of untreated)
0.00	0.79 (100)	0.71 (100)
0.24	0.72 (91)	0.65 (92)
0.64	0.42 (53)	0.35 (49)
1.1	0.30 (38)	0.29 (41)
1.6	0.087 (11)	0.11 (15)
2.1	0.002 (0.2)	<0.001 (<0.14)

[a] Units: μmol of *p*NPP hydrolyzed·min^{-1}·mg^{-1} at 10 mM *p*NPP as described under Experimental Procedures.

effect of dithionite reduction on enzyme activity. The EPR spectrum of this sample prior to the addition of dithionite indicates that the majority of the sample is present in the mixed valence oxidation state as evidenced by the presence of the $g_{av} < 2.0$ EPR resonance (spin quantitation yielded 0.79 spin/mol of protein, Figure 5A). Anaerobic additions of dithionite to this sample resulted in the gradual decrease in intensity of the mixed valence EPR signal (Figure 5B−F; Table 1). During the course of the titration, aliquots were transferred to a quartz cuvette for measurement of phosphatase activity as described under Experimental Procedures, being careful to maintain anaerobic conditions during the transfer and assay period. As can be seen in Table 1, the activity of calcineurin at each stage of the titration parallels the intensity of the EPR resonance due to the mixed valence species with complete abolishment of enzyme activity (<0.14%) following reduction of the mixed valence species.

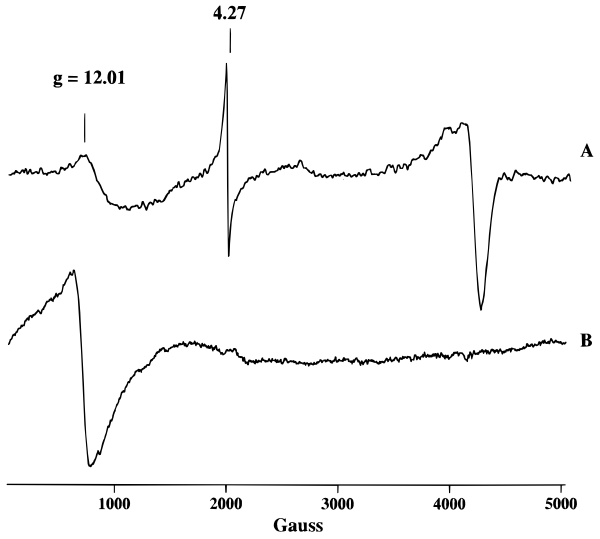

FIGURE 6: Perpendicular (A) and parallel (B) mode EPR spectra of mixed valence iron substituted calcineurin. The 250 μL sample contained 128 μM iron-substituted calcineurin in 100 mM Tris-HCl, pH 7.5 and 100 mM BME. Spectrometer conditions: dual mode resonator; microwave power, 50 mW; microwave frequency, 9.647 GHz (perpendicular mode), 9.348 GHz (parallel mode); modulation amplitude, 10 G at 100 kHz; temperature, 5 K.

The presence of β-mercaptoethanol in the sample buffer required an excess of dithionite to achieve complete reduction. Neither the phosphatase activity nor the intensity of the EPR signal was affected in a parallel sample that was subject to five consecutive freeze/thaw cycles under anaerobic conditions (data not shown).

During dithionite titration, a new resonance with $g \approx 12$ appears and increases in intensity as the dithionite concentration in the sample increases (arrow, Figure 5F). We attribute this resonance to an integer spin system. Transitions between states split by the Zeeman interaction of integer spin systems typically have low transition probabilities and thus weak resonance intensities in a perpendicular mode (microwave field, H_1, perpendicular to the laboratory magnetic field, H_0) EPR cavity. In order to demonstrate that the $g \approx 12$ resonance of dithionite-reduced calcineurin arises from an integer spin system, we recorded EPR spectra of reduced calcineurin in a bimodal cavity which can obtain spectra in either perpendicular or parallel (H_1 parallel to H_0) modes. Integer spin resonances generally have higher transition probabilities, and, hence, stronger intensities, when the microwave field is tuned parallel to the magnetic field. The EPR spectra of a sample of calcineurin exhibiting the $g \approx 12$ resonance recorded in perpendicular and parallel modes are shown in Figure 6. The $g \approx 12$ resonance in the perpendicular mode (Figure 6A) increases in intensity by over a factor of 2.5 when the microwave field is tuned parallel to the magnetic field (Figure 6B), demonstrating that it originates from a paramagnetic component with integer spin.

Oxidation of the Mixed Valence Cluster of Calcineurin by Hydrogen Peroxide. Figure 7 shows EPR spectra of iron-substituted calcineurin prepared in the mixed valence oxidation state treated with various concentrations of hydrogen peroxide. The intensity of the mixed valence signal gradually decreases as the concentration of hydrogen peroxide increases from 0 to 0.96 mM (Figure 7A−E), a result of oxidizing the dinuclear iron center to the diferric ($Fe^{3+}-Fe^{3+}$) oxidation

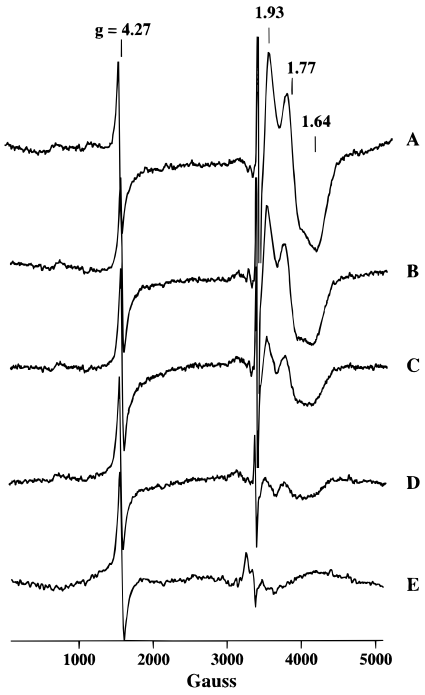

FIGURE 7: EPR spectra of mixed valence iron-substituted calcineurin in the presence of various concentrations of hydrogen peroxide at 3.6 K. The 250 μL sample contained 150 μM iron-substituted calcineurin in 50 mM Tris-HCl, 1 mM BME, pH 7.5. The sample (A) was recorded in the absence of hydrogen peroxide while spectra in (B), (C), (D), and (E) were recorded in the presence of 0.24 mM, 0.48 mM, 0.72 mM, and 0.96 mM hydrogen peroxide, respectively. Spectrometer conditions: microwave frequency, 9.443 GHz; modulation amplitude, 10 G at 100 kHz; microwave power, 20 mW.

Table 2: Correlation between Calcineurin Activity and the Intensity of the Mixed Valence $Fe^{3+}-Fe^{2+}$ EPR Signal during Hydrogen Peroxide Oxidation

$[H_2O_2]$, mM	signal intensity spins per protein (% of untreated)	calcineurin *p*NPP act., units[a] (% of untreated)
0.00	0.814 (100)	0.87 (100)
0.24	0.596 (73)	0.71 (82)
0.48	0.293 (36)	0.38 (44)
0.72	0.114 (14)	0.18 (21)
0.96	0 (0)	0.05 (6)

[a] Units: μmol of *p*NPP hydrolyzed·min^{-1}·mg^{-1} at 10 mM *p*NPP as described under Experimental Procedures.

state. As observed during dithionite reductions, an excess of hydrogen peroxide was required for complete oxidation due to the presence of β-mercaptoethanol in the sample buffer. The decrease in signal intensity of the mixed valence species is coincident with a parallel decrease in phosphatase activity (Table 2) and indicates that the diferric state of the metal cluster represents a catalytically inactive oxidation state.

DISCUSSION

In this study, we have characterized the spectroscopic and catalytic properties of the dinuclear metal cofactor in calcineurin. We thus prepared calcineurin in the "native" $Fe^{3+}-Zn^{2+}$ or "iron-substituted" $Fe^{3+}-Fe^{2+}$ mixed valence forms, characterized each in terms of interaction with product phosphate, and followed the activity of the mixed valence state of iron-substituted calcineurin during either reductive titrations with dithionite or oxidative titrations with hydrogen peroxide. We find that both the $Fe^{3+}-Zn^{2+}$ and $Fe^{3+}-Fe^{2+}$ metal centers of calcineurin exhibit spectroscopic and enzymatic properties which parallel those observed for the corresponding metal clusters of purple acid phosphatases. Although calcineurin, PP1, and PP2A are not "purple" phosphatases (Rusnak et al., 1996), the similarities of their active sites and biochemical properties are compelling evidence that they share a similar catalytic mechanism.

Purple acid phosphatases have been isolated containing two different metal clusters. Kidney bean purple acid phosphatase contains an $Fe^{3+}-Zn^{2+}$ active site cofactor (Sträter et al., 1995), a metal cluster also found in calcineurin isolated from bovine brain (Yu et al., 1995). In contrast, mammalian purple acid phosphatases, which include uteroferrin (Averill et al., 1987), bovine spleen purple acid phosphatase (Averill et al., 1987), and the bone osteoclast tartarate-resistant acid phosphatase (Hayman & Cox, 1994), contain dinuclear iron cofactors which can be obtained in two oxidation states. Aerobic purification results in isolation of mammalian purple acid phosphatase in the purple ($\lambda_{max} \approx 550$ nm) $Fe^{3+}-Fe^{3+}$ state which is catalytically inactive ($\leq$5% activity, vide infra). Treatment of the purple form with mild reductants, e.g., BME or ascorbate, yields the pink form ($\lambda_{max} \approx 510$ nm) that is catalytically active and exhibits an EPR spectrum with *g*-values of 1.94, 1.76, and 1.56 from the dinuclear iron cluster in the mixed valence $Fe^{3+}-Fe^{2+}$ oxidation state (Davis & Averill, 1982; Antanaitis et al., 1980, 1983; Averill et al., 1987). Interconversion between the $Fe^{3+}-Zn^{2+}$ and $Fe^{3+}-Fe^{2+}$ forms in the purple acid phosphatases is readily achieved (Antanaitis et al., 1983; Beck et al., 1988; David & Que, 1990), and this procedure has been used to replace Zn^{2+} in bovine brain calcineurin with Fe^{2+} to yield a dinuclear $Fe^{3+}-Fe^{2+}$ center which also exhibits a mixed valence EPR signal with $g_{av} < 2.0$ (Yu et al., 1995).

As with purple acid phosphatase, calcineurin prepared in the $Fe^{3+}-Fe^{2+}$ oxidation state loses activity upon oxidation. Thus, treatment with H_2O_2 led to a steady decrease in the mixed valence EPR signal with a concomitant decrease in phosphatase activity. When complete oxidation of the mixed valence cluster was achieved as judged by EPR, calcineurin retained 6% activity compared to the mixed valence form of the enzyme. Although the oxidized form of purple acid phosphatase is normally considered to be inactive, some residual activity (5% compared to the activity of the mixed valence form) has been reported and attributed to the diferric oxidation state (Dietrich et al., 1991). Thus, the remaining 6% activity exhibited by calcineurin following oxidation is comparable. Although it is possible that the diferric state of calcineurin is responsible for this residual activity, it is not possible at this time to rule out the presence of a small amount of $Fe^{3+}-Zn^{2+}$ species due to incomplete iron substitution. In fact, an EPR signal from a high-spin Fe^{3+} species with $g = 9.2$ is evident in the sample and undergoes little change during H_2O_2 titration (Figure 7). Although distinct from the EPR signal of the $Fe^{3+}-Zn^{2+}$ form of bovine calcineurin (Figure 1), it may represent the species responsible for the residual activity following oxidation.

In the diiron forms of mammalian purple acid phosphatases, conversion from the oxidized (diferric) to the mixed valence oxidation state can be achieved by the addition of mild reducing agents such as $Fe(NH_4)_2(SO_4)_2$/ascorbate,

BME, or 1 equiv of sodium dithionite/methyl viologen ($E_o' = -440$ mV) (Averill et al., 1987; Schlosnagle et al., 1974). Additional equivalents of dithionite, however, lead to bleaching of the color, loss of the mixed valence EPR resonance, and loss of iron from the sample (Schlosnagle et al., 1976; Averill et al., 1987). In fact, Keough et al. found that approximately half the iron is lost rapidly when purple acid phosphatase is treated with dithionite while the remainder was removed over a period of several hours (Keough et al., 1980). They attributed loss of enzyme activity to result from the conversion to a "one-iron" apoenzyme.

Dithionite reduction of mixed valence iron-substituted calcineurin also led to a loss of activity. However, the appearance of a $g \approx 12$ EPR resonance suggests that loss of activity may not be due solely to loss of one or both of the metal ions of the cluster. The fact that the $g \approx 12$ resonance increases in intensity in a parallel mode cavity firmly establishes that it arises from an integer spin state. The resonance condition for integer spin systems is given by eq 2:

$$(h\nu)^2 = \Delta^2 + (g_{\text{eff}}\beta H)^2 \qquad (2)$$

where Δ represents the splitting between levels of a spin multiplet and g_{eff} represents an effective g-value that is a function of the zero-field splitting and g-tensor terms of the spin Hamiltonian (Hendrich & Debrunner, 1989; Münck et al., 1993). For resonance to occur, the splitting Δ must be smaller than the EPR microwave quantum $h\nu$ ($h\nu \approx 0.3$ cm^{-1} at X-band). The most likely possibility for the origin of this resonance is the diferrous ($Fe^{2+}-Fe^{2+}$) oxidation state produced by a one-electron reduction of the mixed valence cluster. Integer spin EPR resonances from a spin-coupled dinuclear $Fe^{2+}-Fe^{2+}$ cluster with $g \approx 16$ have been observed in methane monooxygenase (Fox et al., 1988; Hendrich et al., 1990) and the azide complex of hemerythrin (Reem & Solomon, 1984; Hendrich & Debrunner, 1989). The $g \approx 12$ resonance therefore may represent a transition between closely spaced levels of a spin-coupled diferrous cluster with $S = 4$ (Hendrich & Debrunner, 1989; Münck et al., 1993). In fact, using Mössbauer spectroscopy, a diferrous cluster has also been implicated in kidney bean purple acid phosphatase following reduction of the diferric enzyme with high concentrations of ascorbate (Suerbaum et al., 1993). Although it is possible that the $g \approx 12$ resonance results from a "one-iron" enzyme, we do not favor this possibility. Integer spin resonances from mononuclear metal sites such as hexaaquo Fe^{2+}, Fe^{2+}−EDTA, and the photodissociated state of (carbonmonoxy)myoglobin occur at higher magnetic fields with $g_{\text{eff}} \leq 8$ (Hendrich & Debrunner, 1989; Münck et al., 1993). Regardless of the fate of the metal ions, it can be concluded that reduction of the $Fe^{3+}-Fe^{2+}$ or $Fe^{3+}-Zn^{2+}$ metal clusters in calcineurin (Yu et al., 1995) leads to loss of activity.

Phosphate inhibits the activity of both calcineurin (Martin & Graves, 1986) and uteroferrin (Keough et al., 1982) by binding to the active site metal center. Recent crystallographic studies of the tungstate complex of PP1 (Egloff et al., 1995), the phosphate complex of calcineurin (Griffith et al., 1995), and the phosphate and tungstate complexes of kidney bean purple acid phosphatase (Klabunde et al., 1996) suggest that inhibition occurs by bidentate coordination of both metal ions of the cluster. EPR and susceptibility (Day et al., 1988), Mössbauer (Pyrz et al., 1986), and EXAFS (Wang et al., 1996b) studies of uteroferrin are also consistent with this mode of inhibition. The addition of phosphate to both the $Fe^{3+}-Zn^{2+}$ and $Fe^{3+}-Fe^{2+}$ forms of calcineurin led to distinct changes in the corresponding EPR signals. The EPR signal of $Fe^{3+}-Zn^{2+}$ calcineurin exhibited minor changes upon phosphate addition, a result that can be explained by a perturbation of the zero-field splitting parameters D and E for the high-spin Fe^{3+} ion of the cluster, most likely by direct coordination of the phosphate oxygen atoms to the metal ions. Given the diamagnetic nature of Zn^{2+}, it is impossible to determine by EPR whether phosphate is interacting with this ion. Additional spectroscopic studies such as ENDOR, EXAFS, or paramagnetic NMR may be able to determine additional structural features regarding the mode of phosphate coordination.

Phosphate addition to the $Fe^{3+}-Fe^{2+}$ form of calcineurin, on the other hand, led to a decrease in intensity and significant broadening of the signal from the mixed valence center. In fact, the EPR relaxation properties of the phosphate complex of calcineurin, such as a tolerance to power saturation at low temperature and an increased sensitivity to temperature, are similar to those observed for the uteroferrin·phosphate complex (Day et al., 1988). With uteroferrin·phosphate, the perturbations of the EPR signal of the mixed valence cluster were explained to result from a decrease in the exchange coupling constant J for the mixed valence cluster, possibly by protonation of the bridging solvent molecule of the cluster. Our results indicate that phosphate inhibition of calcineurin is occurring in a similar fashion.

The reductive and oxidative titrations firmly establish that, at least for the diiron form of calcineurin, the relevant oxidation state of the metal ions is the mixed valence $Fe^{3+}-Fe^{2+}$ state. Thus, treatment with dithionite leads to a loss of activity associated with reduction of the Fe^{3+} ion in the M1 site of the cluster to form a diferrous cluster. The requirement for Fe^{3+} in the M1 site suggests a role for that metal in activating a water molecule for nucleophilic attack since water coordinated to Fe^{3+} is expected to have a lower pK_a than water coordinated to Fe^{2+}. Thus, water coordinated to Fe^{3+} is more readily deprotonated to yield a metal-coordinated hydroxide, the putative nucleophile in the reaction. The corresponding loss of activity upon H_2O_2 oxidation to the diferric state indicates that the M2 site should contain a divalent metal ion, in this case either Fe^{2+} or Zn^{2+}. A divalent metal ion requirement for M2 (versus, for example, Fe^{3+}) may indicate a role in phosphate oxygen coordination during the catalytic cycle. With Fe^{3+} occupying the M2 site, one would expect a higher affinity for phosphate and hence a slower release of product phosphate from the diferric versus mixed valence cluster. In fact, the lower activity of oxidized purple acid phosphatase was interpreted to result not only from slower product release, but also from slower formation of the enzyme·substrate complex (Dietrich et al., 1991).

It is intriguing that native bovine calcineurin is isolated containing $Fe^{3+}-Zn^{2+}$ as active site metals. One possible advantage of maintaining a Zn^{2+} ion in the M2 site of calcineurin, in contrast to a Fe^{2+} ion as in mammalian purple acid phosphatases, would be to prevent oxidation and subsequent inactivation. Interestingly, a recent manuscript has suggested that the active form of calcineurin contains

an Fe^{2+}-Zn^{2+} cluster that undergoes inactivation upon oxidation to the $Fe^{3+}-Zn^{2+}$ state (Wang et al., 1996a). Previous experiments utilizing the native $Fe^{3+}-Zn^{2+}$ enzyme (Yu et al., 1995) as well as the data described herein with iron-substituted $Fe^{3+}-Fe^{2+}$ imply that the mixed valence $Fe^{3+}-M^{2+}$ (M = Fe, Zn) oxidation state is required for catalytic competence. The finding that calcineurin in a crude rat brain preparation was protected from inactivation by ascorbate and could be reactivated by $Fe(NH_4)_2(SO_4)_2$ may indicate that *rat* brain calcineurin contains a dinuclear $Fe^{3+}-Fe^{2+}$ center which would be subject to oxidative inactivation. Experiments to verify this are in progress.

ACKNOWLEDGMENT

We thank Paul Lindahl for providing a schematic for the anaerobic cell and for helpful advice. We also gratefully acknowledge John D. Lipscomb for the use of the Varian EPR spectrometer.

REFERENCES

Aasa, R., & Vänngård, T. (1975) *J. Magn. Reson. 19*, 308.
Antanaitis, B. C., Aisen, P., Lilienthal, H. R., Roberts, R. M., & Bazer, F. W. (1980) *J. Biol. Chem. 255*, 11204.
Antanaitis, B. C., Aisen, P., & Lilienthal, H. R. (1983) *J. Biol. Chem. 258*, 3166.
Averill, B. A., Bale, J. R., & Orme-Johnson, W. H. (1978) *J. Am. Chem. Soc. 100*, 3034.
Averill, B. A., Davis, J. C., Burman, S., Zirino, T., Sanders-Loehr, J., Loehr, T. M., Sage, J. T., & Debrunner, P. G. (1987) *J. Am. Chem. Soc. 109*, 3760.
Beck, J. L., Keough, D. T., De Jersey, J., & Zerner, B. (1984) *Biochim. Biophys. Acta 791*, 357.
Beck, J. L., De Jersey, J., Zerner, B., Hendrich, M. P., & Debrunner, P. G. (1988) *J. Am. Chem. Soc. 110*, 3317.
Bradford, M. M. (1976) *Anal. Biochem. 72*, 248.
David, S. S., & Que, L., Jr. (1990) *J. Am. Chem. Soc. 112*, 6455.
Davis, J. C., & Averill, B. A. (1982) *Proc. Natl. Acad. Sci. U.S.A. 79*, 4623.
Day, E. P., David, S. S., Peterson, J., Dunham, W. R., Bonvoisin, J. J., Sands, R. H., & Que, L., Jr. (1988) *J. Biol. Chem. 263*, 15561.
Dedman, J. R., & Kaetzel, M. A. (1983) *Methods Enzymol. 102*, 1.
Dietrich, M., Münstermann, D., Suerbaum, H., & Witzel, H. (1991) *Eur. J. Biochem. 199*, 105.
Egloff, M.-P., Cohen, P. T. W., Reinemer, P., & Barford, D. (1995) *J. Mol. Biol. 254*, 942.
Fox, B. G., Surerus, K. K., Münck, E., & Lipscomb, J. D. (1988) *J. Biol. Chem. 263*, 10553.
Goldberg, J., Huang, H., Kwon, Y., Greengard, P., Nairn, A. C., & Kuriyan, J. (1995) *Nature 376*, 745.
Griffith, J. P., Kim, J. L., Kim, E. E., Sintchak, M. D., Thomson, J. A., Fitzgibbon, M. J., Fleming, M. A., Caron, P. R., Hsiao, K., & Navia, M. A. (1995) *Cell 82*, 507.
Hayman, A. R., & Cox, T. M. (1994) *J. Biol. Chem. 269*, 1294.
Hendrich, M. P., & Debrunner, P. G. (1989) *Biophys. J. 56*, 489.
Hendrich, M. P., Münck, E., Fox, B. G., & Lipscomb, J. D. (1990) *J. Am. Chem. Soc. 112*, 5861.
Holz, R. C., Que, L., Jr., & Ming, L.-J. (1992) *J. Am. Chem. Soc. 114*, 4434.
Keough, D. T., Dionysius, D. A., De Jersey, J., & Zerner, B. (1980) *Biochem. Biophys. Res. Commun. 94*, 600.
Keough, D. T., Beck, J. L., De Jersey, J., & Zerner, B. (1982) *Biochem. Biophys. Res. Commun. 108*, 1643.
King, M. M., & Huang, C. Y. (1984) *J. Biol. Chem. 259*, 8847.
Kissinger, C. R., Parge, H. E., Knighton, D. R., Lewis, C. T., Pelletier, L. A., Tempczyk, A., Kalish, V. J., Tucker, K. D., Schowalter, R. E., Moomaw, E. W., Gastinel, L. N., Habuka, N., Chen, X., Maldonado, F., Barker, J. E., Bacguet, R., & Villafranca, J. E. (1995) *Nature 378*, 641.
Klabunde, T., Sträter, N., Fröhlich, R., Witzel, H., & Krebs, B. (1996) *J. Mol. Biol. 259*, 737.
Klee, C. B., Krinks, M. H., Manalan, A. S., Cohen, P., & Stewart, A. A. (1983) *Methods Enzymol. 102*, 227.
Koonin, E. V. (1994) *Protein Sci. 3*, 356.
Kurtz, D. M., Jr. (1990) *Chem. Rev. 90*, 585.
Lohse, D. L., Denu, J. M., & Dixon, J. E. (1996) *Structure 3*, 987.
Martin, B. L., & Graves, D. J. (1986) *J. Biol. Chem. 261*, 14545.
Münck, E., Surerus, K. K., & Hendrich, M. P. (1993) *Methods Enzymol. 227*, 463.
Pallen, C. J., & Wang, J. H. (1983) *J. Biol. Chem. 258*, 8550.
Pallen, C. J., & Wang, J. H. (1984) *J. Biol. Chem. 259*, 6134.
Pallen, C. J., & Wang, J. H. (1986) *J. Biol. Chem. 261*, 16115.
Pyrz, J. W., Sage, J. T., Debrunner, P. G., & Que, L., Jr. (1986) *J. Biol. Chem. 261*, 11015.
Rao, J., & Wang, J. H. (1989) *J. Biol. Chem. 264*, 1058.
Reem, R. C., & Solomon, E. I. (1984) *J. Am. Chem. Soc. 106*, 8323.
Rusnak, F., Yu, L., & Mertz, P. (1996) *J. Biol. Inorg. Chem. 1*, 388.
Schlosnagle, D. C., Bazer, F. W., Tsibris, J. C. M., & Roberts, R. M. (1974) *J. Biol. Chem. 249*, 7574.
Schlosnagle, D. C., Sander, E. G., Bazer, F. W., & Roberts, R. M. (1976) *J. Biol. Chem. 251*, 4680.
Shenolikar, S., & Nairn, A. C. (1991) *Adv. Second Messenger Phosphoprotein Res. 23*, 1.
Sikkink, R., Haddy, A., Mackelvie, S., Mertz, P., Litwiller, R., & Rusnak, F. (1995) *Biochemistry 34*, 8348.
Sträter, N., Klabunde, T., Tucker, P., Witzel, H., & Krebs, B. (1995) *Science 286*, 1489.
Suerbaum, H., Körner, M., Witzel, H., Althaus, E., Mosel, B.-D., & Müller-Warmuth, W. (1993) *Eur. J. Biochem. 214*, 313.
Vincent, J. B., Olivier-Lilley, G. L., & Averill, B. A. (1990) *Chem. Rev. 90*, 1447.
Wang, X., Culotta, V. C., & Klee, C. B. (1996a) *Nature 383*, 434.
Wang, X., Randall, C. R., True, A. E., & Que, L., Jr. (1996b) *Biochemistry 35*, 13946.
Yu, L., Haddy, A., & Rusnak, F. (1995) *J. Am. Chem. Soc. 117*, 10147.
Zhang, J., Zhang, Z., Brew, K., & Lee, E. Y. C. (1996) *Biochemistry 35*, 6276.
Zhuo, S., Clemens, J. C., Hakes, D. J., Barford, D., & Dixon, J. E. (1993) *J. Biol. Chem. 268*, 17754.
Zhuo, S., Clemens, J. C., Stone, R. L., & Dixon, J. E. (1994) *J. Biol. Chem. 269*, 26234.

BI970519G